Coffee ring effect during drying of colloid drop. Experiment and computer simulation

V. Ya. Shur[1], D. A. Bykov[1,2], E. A. Mingaliev[1], A. E. Tyurnina[1,3], G. V. Burban[1], R. M. Kadushnikov[2], V. V. Mizgulin[2]

[1]Institute of Natural Sciences, Ural Federal University, 620000 Ekaterinburg, Russia

[2]SIAMS Ltd., 620078 Ekaterinburg, Russia

[3]UNIIM, 620000 Ekaterinburg, Russia

Formation of the ring-like patterns of silver nanoparticles (NPs) during drying of colloid drop caused by coffee ring effect has been studied experimentally and by computer simulation. The drop shape evolution during jump-like motion of its contact line was *in situ* observed. Two interleaved stages of the drop shape evolution were separated for computer simulation. The even stages represent decreasing of drop height at constant base radius and the odd stages – the fast shift of the contact line at the constant volume. The proposed model allows extracting the parameters characterizing formation of NPs pattern during drying of colloid drop.

Keywords: drop drying, nanoparticles, self-assembling, self-organization

Short title: Coffee ring effect during drying of colloid drop

Corresponding author: ea.mingaliev@urfu.ru

1. Introduction

The evaporation of a sessile liquid drop, which is important in many heat transfer applications, is associated also with “coffee ring” effect named for the characteristic ring-like patterns formed on the surface after drying of spilled coffee. When the spilled drop of coffee is drying on a solid surface, it leaves a dense ring-like deposit along the perimeter. The coffee, initially dispersed over the entire drop, becomes concentrated in a tiny fraction of it [1].

Nowadays, the applications of this effect for surface-patterning have emerged [2]. As a result of drying of colloid drop deposited on the substrate, the solute particles are deposited on the solid surface, mostly along the drop edge (perimeter). Different patterns can appear on the substrate in various experimental conditions [3-5]. A number of papers devoted to investigation of the nanoparticles (NPs) behavior in a drying drop were published during the last two decades [1, 6-9]. The formation of patterns consisted of nested rings is explained by two main phenomena. The first, known as contact-angle hysteresis, connects with multiple minima of the free energy of a drop deposited on a solid substrate and leads to contact line pinning during evaporation [10-13]. The second is capillary outward flow of solvent in the droplet induced by faster solvent evaporation near the pinned contact line [1, 14]. The thermal and concentration gradients caused by evaporation can lead to circulating flows driven by surface-tension gradients (Marangoni flows [15]).

Recently, the domain kinetics during cyclic switching using stable suspension of Ag NPs as the liquid electrodes has been studied in single crystals of the relaxor ferroelectric strontium-barium niobate $Sr_{0.61}Ba_{0.39}Nb_2O_6$ [16]. The acceleration of the fatigue effect has been revealed. Moreover, the metal NPs deposited on the polar surface of the ferroelectric

crystal can increase the nucleation probability. This effect allows us to predict the qualitative change of the domain kinetics with increasing of the NPs concentration.

The coffee ring effect can be used for controlled creation of the patterns with various spatial distributions of the NPs from uniform micron-scale circles to rings [5]. The self-assembled formation of the quasi-regular nanoscale patterns can be used for creation of the structured electrode for studying the influence of metal NPs on the domain kinetics.

In this paper, the formation of the inhomogeneous NPs patterns during drop drying caused by coffee ring effect has been studied both experimentally and by computer simulation. The proposed model of jump-like motion of the contact line correlates with experimental data.

2. Experimental

The stable colloid of silver NPs has been produced by laser ablation in liquid [17]. The metal target (polished 3-mm-thick plate of pure silver) covered by layer of pure deionized water has been evaporated by focused beam of the Yb fiber infrared laser (wavelength 1064 nm, pulse duration 100 ns, pulse energy 1 mJ, frequency 21 kHz). The charged spherically shaped NPs appeared in the water as a result of condensation [18].

The NPs have been deposited on the substrates by two alternative methods. In the first method, the colloid drops with volume about 5 μl and average diameter above 1 mm were produced by single channel microliter pipette. In the second method, the colloid droplets with pico- or femtoliter volume and corresponding diameter about 10 μm were deposited using pyroelectrohydrodynamic shooting [19]. The drops and droplets placed on the glass substrates have been dried in ambient conditions. The obtained NPs patterns have been visualized by optical microscopy (Fig. 1).

The inhomogeneous structure consisting of enclosed (nested) macro-rings was formed as a result of drop drying (Fig. 1a). In situ observation of the drop shape evolution allows revealing the jump-like motion of the contact line caused by pinning by the NPs on the substrate surface [6]. Two interleave stages of the drop evolution have been revealed. During the first stage, the initial drop height (Fig. 2a) decreases slowly, whereas the contact line is fixed and significant decrease of the wetting angle is observed (Fig. 2b). The fast drop shrinkage at the second stage leads to increase of its height until recovery of the initial value of the wetting angle (Fig. 2c).

Two alternative patterns appeared as a result of colloid droplet drying have been revealed for various NPs concentrations. The formation of the nested rings was obtained for high NPs concentration about 0.5 g/l (Fig. 1b), whereas the uniform distribution of NPs appeared for concentration about 0.1 g/l (Fig. 1c).

3. Modeling

The drop evolution during drying has been studied numerically. The simple model has been considered for explanation of the observed jump-like motion of the contact line. We assume that the drop geometry at every moment represents a spherical segment and can be characterized by radius *R*, height h, and base radius r (Fig. 3). The diffusion of the solution vapor to atmosphere is considered as the only mechanism of the drop drying. Two interleaved stages of the drop shape evolution during drying are separated. The first and all subsequent even stages correspond to slow drop volume reduction due to decreasing of *h* at constant *r*. The second and all subsequent odd stages represent the fast shift of the contact line (abrupt decrease of *r* and increase of *h*) at constant drop volume. The transitions from odd stages to the even ones are obtained, when relation h/r_n achieves the critical value $(h/r)_{cr}$. The sequence

of odd and even stages leads to jump-like motion of the contact line characterized by the series of the base radii r_n corresponding to stay positions of the contact line.

The rate of drop volume decrease (drying rate) at the odd stages is proportional to the area of the liquid-vapor interface at given moment *S(t)*. Let us define the volume change per time step as follows:

$$\Delta V = -\alpha\, S(t)\, \Delta t \tag{1}$$

where α is the drying rate per surface unit, Δt is the integration step.

For spherical segment:

$$\Delta V = -\pi\alpha\, (r^2 + h^2)\, \Delta t \tag{2}$$

At every step of iteration *i* the value of the drop volume computes as $V_i = V_{i-1} - \Delta V_{i-1}$. In assumption that the drop geometry is the spherical segment, from the known value of the volume computes the height of the drop h_i. The volume of the spherical segment of the radius R is equal:

$$V = \pi\, h^2\, (R - h/3) \tag{3}$$

It is known that $R = (r^2 + h^2)/2h$. Thus, we can write:

$$h^3 + 3\, r^2 h - 6\, V/\pi = 0 \tag{4}$$

The solution of the Eq. (4) allows obtaining the height of the drop:

$$h = \sqrt[3]{3\,V/\pi + \sqrt{r^6 + 9\,V^2/\pi^2}} + \sqrt[3]{3\,V/\pi - \sqrt{r^6 + 9\,V^2/\pi^2}} \tag{5}$$

When h_i/r_n achieves the critical value $(h/r)_{cr}$, the second (even) stage of the drying process occurs. In simulations we neglect the duration of even stages, because they are much shorter than the odd stages. Thus, we compute the new drop base radius r_{n+1} in one iteration. At the beginning of each odd stage h_o/r_{n+1} is equal to the constant value $(h/r)_{st}$.

It is necessary to point out that the initial shape parameter of the drop $(h/r)_o$, which is always noticeably larger than $(h/r)_{st}$, can be measured experimentally. Three free parameters of the model have been used for fitting of the experimental data: $(h/r)_{cr}$, $(h/r)_{st}$, and α.

The rings of the NPs appeared for jump-like motion of the contact line at all stay positions due to acceleration of the NPs segmentation at the drop edge during drying of the colloid drop [14].

4. Results and discussion

We have measured the evolution of the shape parameters of the drying colloid drop of Ag NPs with concentration of 0.1 g/l. The obtained experimental data were compared with results of the computer simulation (Fig. 2). The initial drop height and the radius of the drop base were about 490 μm and 700 μm, respectively, which corresponds to $(h/r)_o$ = 0.7. The total drying time at ambient conditions was about 570 seconds.

The NPs pattern on the substrate after drop drying is represented in Fig. 4. Results of the computer simulation (Fig. 4a) were compared with the experimental data (Fig. 4b). It is seen that the shape of the experimental rings deviates significantly from the circular. Thus, the effective radii were calculated from the areas: $r_n = (A_n/\pi)^{0.5}$.

The fitting of the experimental data allowed to reveal the crytical value of the shape parameter $(h/r)_{cr}$, = 0.2, the start value of the shape parameter $(h/r)_{st}$ = 0.34, and relative drying rate per surface unit α = 0.75 μm/s.

The simulated time dependence of the drop radius is represented in Fig. 5a. The horizontal sections correspond to the drop drying stages with a fixed contact line (odd stages), and the vertical ones – to the contact line shifts (even stages). The decreasing of the duration of odd stages leads to termination of the ring formation mechanism. It means that the

particles were deposited on the substrate more uniformly. Such stage is obtained experimentally (Fig. 4b).

The comparison of the simulated drop base radii r_n and the experimentally observed effective radii of the NPs rings (Fig. 5b) confirms that the proposed model can be used for analysis of the experimental data and allows to extract the important parameters characterizing the formation of the NPs pattern during drying of colloid drop.

5. Conclusion

The formation of the patterns of Ag NPs consisting of enclosed macro-rings during drying of colloid drop caused by coffee ring effect has been studied both experimentally and by computer simulation. In situ observation of the shape evolution of drying drop allowed us to reveal the jump-like motion of the contact line. The formation of the nested rings was obtained for NPs concentration about 0.5 g/l, whereas the uniform distribution of NPs appeared for concentration about 0.1 g/l. Two interleaved stages of the drop shape evolution during drying were separated for computer simulation. The first and all subsequent even stages corresponded to slow drop volume reduction due to decreasing of drop height at constant base radius. The second and all subsequent odd stages represented the fast shift of the contact line at constant drop volume. The transitions from odd stages to the even ones were obtained, when the drop shape parameter achieved the critical value. The sequence of odd and even stages led to jump-like motion of the contact line characterized by series of the base radii. The proposed model allowed extracting the important parameters characterizing the formation of the NPs pattern during drying of colloid drop.

Acknowledgements

The equipment of the Ural Center for Shared Use “Modern Nanotechnology”, Ural Federal University has been used. The research was made possible in part by the Ministry of Education and Science of the Russian Federation (grants No. 14.594.21.0011 and No. 2457) and RFBR and the Government of Sverdlovsk region (grant 13-02-96041-r-Ural-a).

References

1. Deegan RD, Bakajin O, Dupont TF: Capillary flow as the cause of ring stains from dried liquid drops. Lett. Nat. 1997; 389: 827-829.

2. Dugas V, Broutin J, Souteyrand E: Droplet evaporation study applied to DNA chip manufacturing. Langmuir. 2005; 21: 9130-9136.

3. Latterini L, Blossey R, Hofkens J, Vanoppen P, De Schryver FC, Rowan AE, Nolte RJM: Ring formation in evaporating porphyrin derivative solutions. Langmuir. 1999; 15: 3582-3588.

4. Deegan R, Bakajin O, Dupont T, Huber G, Nagel S, Witten T: Contact line deposits in an evaporating drop. Phys. Rev. E. 2000; 62: 756-765.

5. Widjaja E, Harris MT: Particle deposition study during sessile drop evaporation. AIChE J. 2008; 54: 2250-2260.

6. Adachi E, Dimitrov AS, Nagayama K: Stripe patterns formed on a glass surface during droplet evaporation. Langmuir. 1995; 11: 1057-1060.

7. Rabani E, Reichman DR, Geissler PL, Brus LE: Drying-mediated self-assembly of nanoparticles. Nature. 2003; 426: 271-274.

8. Govor L, Reiter G, Parisi J, Bauer G: Self-assembled nanoparticle deposits formed at the contact line of evaporating micrometer-size droplets. Phys. Rev. E. 2004; 69: 061609.

9. Bigioni TP, Lin XM, Nguyen TT, Corwin EI, Witten TA, Jaeger HM: Kinetically driven self assembly of highly ordered nanoparticle monolayers. Nat. Mater. 2006; 5: 265-270.

10. Shanahan MER: Simple theory of “stick-slip” wetting hysteresis. Langmuir. 1995; 11: 1041-1043.

11. Hu H, Larson RG: Evaporation of a sessile droplet on a substrate. J. Phys. Chem. B.

2002; 106: 1334-1344.

12. Marmur A: Soft contact: measurement and interpretation of contact angles. Soft Matter. 2006; 2: 12-17.

13. Bormashenko E, Musin A, Zinigrad M: Evaporation of droplets on strongly and weakly pinning surfaces and dynamics of the triple line. Colloids Surfaces A. Physicochem. Eng. Asp. 2011; 385: 235-240.

14. Fischer BJ: Particle convection in an evaporating colloidal droplet. Langmuir. 2002; 18: 60-67.

15. Scriven LE, Sterling CV: The Marangoni effects. Nature. 1960; 187: 186-188.

16. Tyurnina AE, Shur VY, Kozin RV, Shikhova VA, Kuznetsov DK, Mingaliev EA, Pelegov DV, Pinegina OA, Ivleva LI: Study of domain kinetics in SBN single crystals in electric field applied by suspension of silver nanoparticles. Ferroelectrics. 2013; 443: 45-53.

17. Tyurnina AE, Shur VY, Kozin RV, Kuznetsov DK, Mingaliev EA: Synthesis of stable silver colloids by laser ablation in water. Proc. SPIE 9065, Fundam. Laser Assist. Micro-Nanotech. 2013; 90650D.

18. Amendola V, Meneghetti M: Laser ablation synthesis in solution and size manipulation of noble metal nanoparticles. Phys. Chem. Chem. Phys. 2009; 11: 3805-3821.

19. Shur VYa, Mingaliev EA, Zorikhin DV, Kosobokov MS, Makaev AV: Generation of picoliter droplets by pyroelectrodynamic effect. Ferroelectrics. 2015; current issue.

Figure captions

Fig. 1. NPs patterns after drying: (a) drop with concentration 0.1 g/l; droplets with concentration (b) 0.1 g/l and (c) 0.5 g/l.

Fig. 2. Optical images of the drop evolution during drying: (a) initial state (t = 0), (b) critical state before the first fast shift of the contact line (t = 261 s), (c) state after the first shift of the contact line (t = 264 s).

Fig. 3. Schematic representation of the drop shape.

Fig. 4. NPs pattern on the substrate after drop drying: (a) computer simulation and (b) experiment.

Fig. 5. (a) The time dependence of the drop base radius obtained by computer simulation. (b) Comparison of the simulated drop base radii r_n (blue squares) and the experimentally observed effective radii of the NPs rings (red dots).

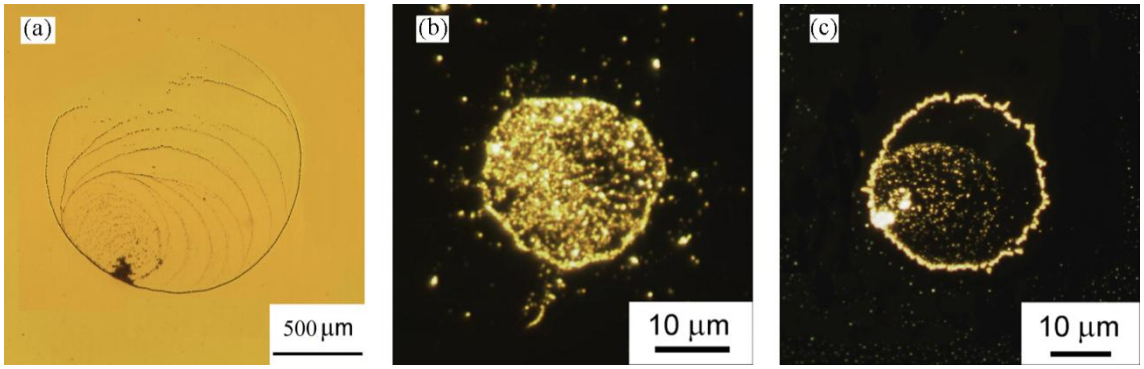

Fig. 1.

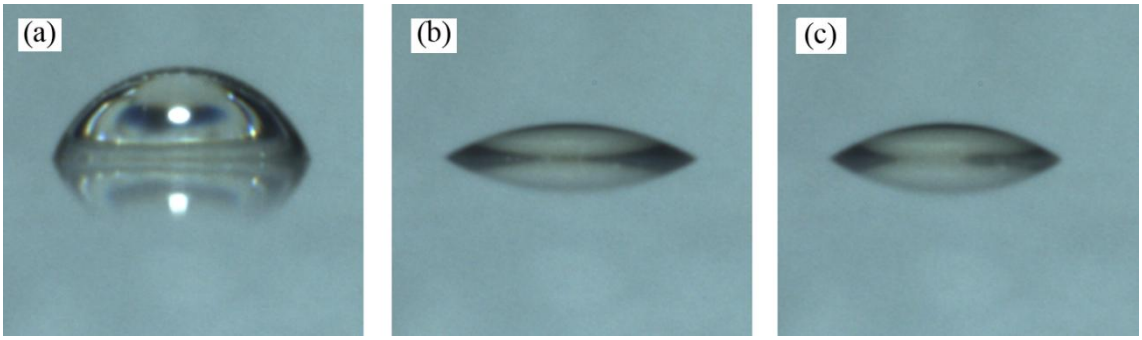

Fig. 2.

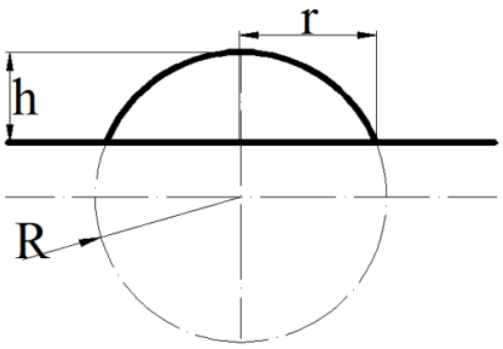

Fig. 3.

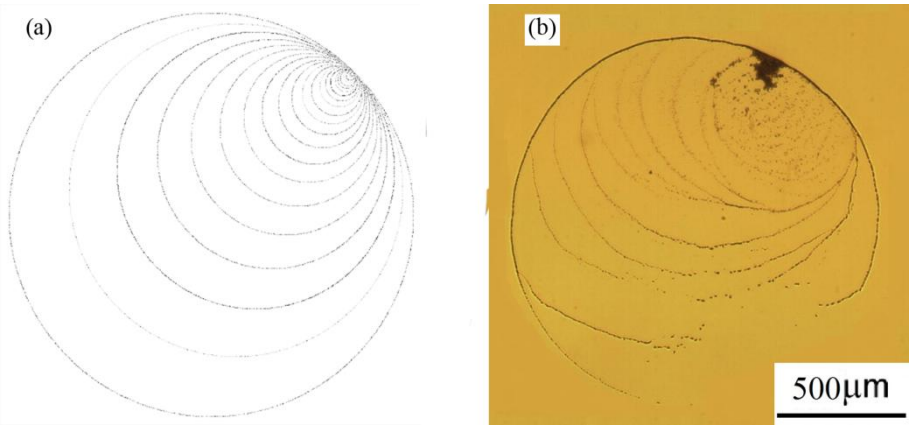
(a)
(b)
500μm

Fig. 4.

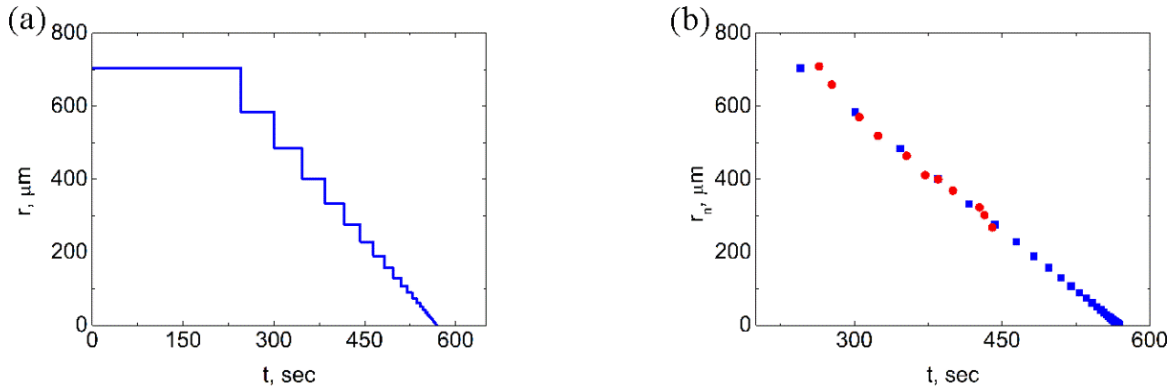
(a)
800
600
400
200
0
r, μm
0
150
300
450
600
t, sec
(b)
800
600
400
200
0
r_n, μm
300
450
600
t, sec

Fig. 5.